

Measurement of the $B^0\bar{B}^0$ oscillation frequency using π - B meson charge-flavor correlations in $p\bar{p}$ collisions at $\sqrt{s} = 1.8$ TeV

F. Abe,¹⁷ H. Akimoto,³⁹ A. Akopian,³¹ M. G. Albrow,⁷ A. Amadon,⁵ S. R. Amendolia,²⁷ D. Amidei,²⁰ J. Antos,³³ S. Aota,³⁷ G. Apollinari,³¹ T. Arisawa,³⁹ T. Asakawa,³⁷ W. Ashmanskas,¹⁸ M. Atac,⁷ P. Azzi-Bacchetta,²⁵ N. Bacchetta,²⁵ S. Bagdasarov,³¹ M. W. Bailey,²² P. de Barbaro,³⁰ A. Barbaro-Galtieri,¹⁸ V. E. Barnes,²⁹ B. A. Barnett,¹⁵ M. Barone,⁹ G. Bauer,¹⁹ T. Baumann,¹¹ F. Bedeschi,²⁷ S. Behrends,³ S. Belforte,²⁷ G. Bellettini,²⁷ J. Bellinger,⁴⁰ D. Benjamin,³⁵ J. Bensinger,³ A. Beretvas,⁷ J. P. Berge,⁷ J. Berryhill,⁵ S. Bertolucci,⁹ S. Bettelli,²⁷ B. Bevensee,²⁶ A. Bhatti,³¹ K. Biery,⁷ C. Bigongiari,²⁷ M. Binkley,⁷ D. Bisello,²⁵ R. E. Blair,¹ C. Blocker,³ S. Blusk,³⁰ A. Bodek,³⁰ W. Bokhari,²⁶ G. Bolla,²⁹ Y. Bonushkin,⁴ D. Bortoletto,²⁹ J. Boudreau,²⁸ L. Breccia,² C. Bromberg,²¹ N. Bruner,²² R. Brunetti,² E. Buckley-Geer,⁷ H. S. Budd,³⁰ K. Burkett,²⁰ G. Busetto,²⁵ A. Byon-Wagner,⁷ K. L. Byrum,¹ M. Campbell,²⁰ A. Caner,²⁷ W. Carithers,¹⁸ D. Carlsmith,⁴⁰ J. Cassada,³⁰ A. Castro,²⁵ D. Cauz,³⁶ A. Cerri,²⁷ P. S. Chang,³³ P. T. Chang,³³ H. Y. Chao,³³ J. Chapman,²⁰ M. -T. Cheng,³³ M. Chertok,³⁴ G. Chiarelli,²⁷ C. N. Chiou,³³ L. Christofek,¹³ M. L. Chu,³³ S. Cihangir,⁷ A. G. Clark,¹⁰ M. Cobal,²⁷ E. Cocca,²⁷ M. Contreras,⁵ J. Conway,³² J. Cooper,⁷ M. Cordelli,⁹ D. Costanzo,²⁷ C. Couyoumtzelis,¹⁰ D. Cronin-Hennessy,⁶ R. Culbertson,⁵ D. Dagenhart,³⁸ T. Daniels,¹⁹ F. DeJongh,⁷ S. Dell’Agnello,⁹ M. Dell’Orso,²⁷ R. Demina,⁷ L. Demortier,³¹ M. Deninno,² P. F. Derwent,⁷ T. Devlin,³² J. R. Dittmann,⁶ S. Donati,²⁷ J. Done,³⁴ T. Dorigo,²⁵ N. Eddy,²⁰ K. Einsweiler,¹⁸ J. E. Elias,⁷ R. Ely,¹⁸ E. Engels, Jr.,²⁸ D. Errede,¹³ S. Errede,¹³ Q. Fan,³⁰ R. G. Feild,⁴¹ Z. Feng,¹⁵ C. Ferretti,²⁷ I. Fiori,² B. Flaugher,⁷ G. W. Foster,⁷ M. Franklin,¹¹ J. Freeman,⁷ J. Friedman,¹⁹ Y. Fukui,¹⁷ S. Galeotti,²⁷ M. Gallinaro,²⁶ O. Ganel,³⁵ M. Garcia-Sciveres,¹⁸ A. F. Garfinkel,²⁹ C. Gay,⁴¹ S. Geer,⁷ D. W. Gerdes,¹⁵ P. Giannetti,²⁷ N. Giokaris,³¹ P. Giromini,⁹ G. Giusti,²⁷ M. Gold,²² A. Gordon,¹¹ A. T. Goshaw,⁶ Y. Gotra,²⁵ K. Goulianos,³¹ H. Grassmann,³⁶ L. Groer,³²

C. Grosso-Pilcher,⁵ G. Guillian,²⁰ J. Guimaraes da Costa,¹⁵ R. S. Guo,³³ C. Haber,¹⁸
E. Hafen,¹⁹ S. R. Hahn,⁷ R. Hamilton,¹¹ T. Handa,¹² R. Handler,⁴⁰ F. Happacher,⁹ K. Hara,³⁷
A. D. Hardman,²⁹ R. M. Harris,⁷ F. Hartmann,¹⁶ J. Hauser,⁴ E. Hayashi,³⁷ J. Heinrich,²⁶
W. Hao,³⁵ B. Hinrichsen,¹⁴ K. D. Hoffman,²⁹ M. Hohlmann,⁵ C. Holck,²⁶ R. Hollebeek,²⁶
L. Holloway,¹³ Z. Huang,²⁰ B. T. Huffman,²⁸ R. Hughes,²³ J. Huston,²¹ J. Huth,¹¹
H. Ikeda,³⁷ M. Incagli,²⁷ J. Incandela,⁷ G. Introzzi,²⁷ J. Iwai,³⁹ Y. Iwata,¹² E. James,²⁰
H. Jensen,⁷ U. Joshi,⁷ E. Kajfasz,²⁵ H. Kambara,¹⁰ T. Kamon,³⁴ T. Kaneko,³⁷ K. Karr,³⁸
H. Kasha,⁴¹ Y. Kato,²⁴ T. A. Keaffaber,²⁹ K. Kelley,¹⁹ R. D. Kennedy,⁷ R. Kephart,⁷
D. Kestenbaum,¹¹ D. Khazins,⁶ T. Kikuchi,³⁷ B. J. Kim,²⁷ H. S. Kim,¹⁴ S. H. Kim,³⁷
Y. K. Kim,¹⁸ L. Kirsch,³ S. Klimenko,⁸ D. Knoblauch,¹⁶ P. Koehn,²³ A. Köngeter,¹⁶
K. Kondo,³⁷ J. Konigsberg,⁸ K. Kordas,¹⁴ A. Korytov,⁸ E. Kovacs,¹ W. Kowald,⁶ J. Kroll,²⁶
M. Kruse,³⁰ S. E. Kuhlmann,¹ E. Kuns,³² K. Kurino,¹² T. Kuwabara,³⁷ A. T. Laasanen,²⁹
I. Nakano,¹² S. Lami,²⁷ S. Lammel,⁷ J. I. Lamoureux,³ M. Lancaster,¹⁸ M. Lanzoni,²⁷
G. Latino,²⁷ T. LeCompte,¹ S. Leone,²⁷ J. D. Lewis,⁷ P. Limon,⁷ M. Lindgren,⁴ T. M. Liss,¹³
J. B. Liu,³⁰ Y. C. Liu,³³ N. Lockyer,²⁶ O. Long,²⁶ C. Loomis,³² M. Loreti,²⁵ D. Lucchesi,²⁷
P. Lukens,⁷ S. Lusin,⁴⁰ J. Lys,¹⁸ K. Maeshima,⁷ P. Maksimovic,¹⁹ M. Mangano,²⁷
M. Mariotti,²⁵ J. P. Marriner,⁷ A. Martin,⁴¹ J. A. J. Matthews,²² P. Mazzanti,² P. McIntyre,³⁴
P. Melese,³¹ M. Menguzzato,²⁵ A. Menzione,²⁷ E. Meschi,²⁷ S. Metzler,²⁶ C. Miao,²⁰
T. Miao,⁷ G. Michail,¹¹ R. Miller,²¹ H. Minato,³⁷ S. Miscetti,⁹ M. Mishina,¹⁷ S. Miyashita,³⁷
N. Moggi,²⁷ E. Moore,²² Y. Morita,¹⁷ A. Mukherjee,⁷ T. Muller,¹⁶ P. Murat,²⁷ S. Murgia,²¹
H. Nakada,³⁷ I. Nakano,¹² C. Nelson,⁷ D. Neuberger,¹⁶ C. Newman-Holmes,⁷ C.-Y. P. Ngan,¹⁹
L. Nodulman,¹ S. H. Oh,⁶ T. Ohmoto,¹² T. Ohsugi,¹² R. Oishi,³⁷ M. Okabe,³⁷ T. Okusawa,²⁴
J. Olsen,⁴⁰ C. Pagliarone,²⁷ R. Paoletti,²⁷ V. Papadimitriou,³⁵ S. P. Pappas,⁴¹ N. Parashar,²⁷
A. Parri,⁹ J. Patrick,⁷ G. Pauletta,³⁶ M. Paulini,¹⁸ A. Perazzo,²⁷ L. Pescara,²⁵ M. D. Peters,¹⁸
T. J. Phillips,⁶ G. Piacentino,²⁷ M. Pillai,³⁰ K. T. Pitts,⁷ R. Plunkett,⁷ L. Pondrom,⁴⁰
J. Proudfoot,¹ F. Ptohos,¹¹ G. Punzi,²⁷ K. Ragan,¹⁴ D. Reher,¹⁸ M. Reischl,¹⁶ A. Ribon,²⁵
F. Rimondi,² L. Ristori,²⁷ W. J. Robertson,⁶ T. Rodrigo,²⁷ S. Rolli,³⁸ L. Rosenson,¹⁹
R. Roser,¹³ T. Saab,¹⁴ W. K. Sakumoto,³⁰ D. Saltzberg,⁴ A. Sansoni,⁹ L. Santi,³⁶

H. Sato,³⁷ P. Schlabach,⁷ E. E. Schmidt,⁷ M. P. Schmidt,⁴¹ A. Scott,⁴ A. Scribano,²⁷ S. Segler,⁷ S. Seidel,²² Y. Seiya,³⁷ F. Semeria,² T. Shah,¹⁹ M. D. Shapiro,¹⁸ N. M. Shaw,²⁹ P. F. Shepard,²⁸ T. Shibayama,³⁷ M. Shimojima,³⁷ M. Shochet,⁵ J. Siegrist,¹⁸ A. Sill,³⁵ P. Sinervo,¹⁴ P. Singh,¹³ K. Sliwa,³⁸ C. Smith,¹⁵ F. D. Snider,¹⁵ J. Spalding,⁷ T. Speer,¹⁰ P. Sphicas,¹⁹ F. Spinella,²⁷ M. Spiropulu,¹¹ L. Spiegel,⁷ L. Stanco,²⁵ J. Steele,⁴⁰ A. Stefanini,²⁷ R. Ströhmer,^{7a} J. Strologas,¹³ F. Strumia,¹⁰ D. Stuart,⁷ K. Sumorok,¹⁹ J. Suzuki,³⁷ T. Suzuki,³⁷ T. Takahashi,²⁴ T. Takano,²⁴ R. Takashima,¹² K. Takikawa,³⁷ M. Tanaka,³⁷ B. Tannenbaum,²² F. Tartarelli,²⁷ W. Taylor,¹⁴ M. Tecchio,²⁰ P. K. Teng,³³ Y. Teramoto,²⁴ K. Terashi,³⁷ S. Tether,¹⁹ D. Theriot,⁷ T. L. Thomas,²² R. Thurman-Keup,¹ M. Timko,³⁸ P. Tipton,³⁰ A. Titov,³¹ S. Tkaczyk,⁷ D. Toback,⁵ K. Tollefson,¹⁹ A. Tollestrup,⁷ H. Toyoda,²⁴ W. Trischuk,¹⁴ J. F. de Troconiz,¹¹ S. Truitt,²⁰ J. Tseng,¹⁹ N. Turini,²⁷ T. Uchida,³⁷ F. Ukegawa,²⁶ S. C. van den Brink,²⁸ S. Vejcik, III,²⁰ G. Velez,²⁷ R. Vidal,⁷ R. Vilar,^{7a} D. Vucinic,¹⁹ R. G. Wagner,¹ R. L. Wagner,⁷ J. Wahl,⁵ N. B. Wallace,²⁷ A. M. Walsh,³² C. Wang,⁶ C. H. Wang,³³ M. J. Wang,³³ A. Warburton,¹⁴ T. Watanabe,³⁷ T. Watts,³² R. Webb,³⁴ C. Wei,⁶ H. Wenzel,¹⁶ W. C. Wester, III,⁷ A. B. Wicklund,¹ E. Wicklund,⁷ R. Wilkinson,²⁶ H. H. Williams,²⁶ P. Wilson,⁵ B. L. Winer,²³ D. Winn,²⁰ D. Wolinski,²⁰ J. Wolinski,²¹ S. Worm,²² X. Wu,¹⁰ J. Wyss,²⁷ A. Yagil,⁷ W. Yao,¹⁸ K. Yasuoka,³⁷ G. P. Yeh,⁷ P. Yeh,³³ J. Yoh,⁷ C. Yosef,²¹ T. Yoshida,²⁴ I. Yu,⁷ A. Zanetti,³⁶ F. Zetti,²⁷ and S. Zucchelli²

(CDF Collaboration)

¹ *Argonne National Laboratory, Argonne, Illinois 60439*

² *Istituto Nazionale di Fisica Nucleare, University of Bologna, I-40127 Bologna, Italy*

³ *Brandeis University, Waltham, Massachusetts 02254*

⁴ *University of California at Los Angeles, Los Angeles, California 90024*

⁵ *University of Chicago, Chicago, Illinois 60637*

⁶ *Duke University, Durham, North Carolina 27708*

⁷ *Fermi National Accelerator Laboratory, Batavia, Illinois 60510*

- ⁸ *University of Florida, Gainesville, FL 32611*
- ⁹ *Laboratori Nazionali di Frascati, Istituto Nazionale di Fisica Nucleare, I-00044 Frascati, Italy*
- ¹⁰ *University of Geneva, CH-1211 Geneva 4, Switzerland*
- ¹¹ *Harvard University, Cambridge, Massachusetts 02138*
- ¹² *Hiroshima University, Higashi-Hiroshima 724, Japan*
- ¹³ *University of Illinois, Urbana, Illinois 61801*
- ¹⁴ *Institute of Particle Physics, McGill University, Montreal H3A 2T8, and University of Toronto,
Toronto M5S 1A7, Canada*
- ¹⁵ *The Johns Hopkins University, Baltimore, Maryland 21218*
- ¹⁶ *Institut für Experimentelle Kernphysik, Universität Karlsruhe, 76128 Karlsruhe, Germany*
- ¹⁷ *National Laboratory for High Energy Physics (KEK), Tsukuba, Ibaraki 305, Japan*
- ¹⁸ *Ernest Orlando Lawrence Berkeley National Laboratory, Berkeley, California 94720*
- ¹⁹ *Massachusetts Institute of Technology, Cambridge, Massachusetts 02139*
- ²⁰ *University of Michigan, Ann Arbor, Michigan 48109*
- ²¹ *Michigan State University, East Lansing, Michigan 48824*
- ²² *University of New Mexico, Albuquerque, New Mexico 87131*
- ²³ *The Ohio State University, Columbus, OH 43210*
- ²⁴ *Osaka City University, Osaka 588, Japan*
- ²⁵ *Universita di Padova, Istituto Nazionale di Fisica Nucleare, Sezione di Padova, I-36132 Padova, Italy*
- ²⁶ *University of Pennsylvania, Philadelphia, Pennsylvania 19104*
- ²⁷ *Istituto Nazionale di Fisica Nucleare, University and Scuola Normale Superiore of Pisa, I-56100 Pisa, Italy*
- ²⁸ *University of Pittsburgh, Pittsburgh, Pennsylvania 15260*
- ²⁹ *Purdue University, West Lafayette, Indiana 47907*
- ³⁰ *University of Rochester, Rochester, New York 14627*
- ³¹ *Rockefeller University, New York, New York 10021*
- ³² *Rutgers University, Piscataway, New Jersey 08855*
- ³³ *Academia Sinica, Taipei, Taiwan 11530, Republic of China*
- ³⁴ *Texas A&M University, College Station, Texas 77843*

³⁵ *Texas Tech University, Lubbock, Texas 79409*

³⁶ *Istituto Nazionale di Fisica Nucleare, University of Trieste/ Udine, Italy*

³⁷ *University of Tsukuba, Tsukuba, Ibaraki 315, Japan*

³⁸ *Tufts University, Medford, Massachusetts 02155*

³⁹ *Waseda University, Tokyo 169, Japan*

⁴⁰ *University of Wisconsin, Madison, Wisconsin 53706*

⁴¹ *Yale University, New Haven, Connecticut 06520*

We present a measurement of the $B^0 \leftrightarrow \bar{B}^0$ oscillation frequency using a flavor tagging method based on correlations of B meson flavor with the charge of other particles produced in $p\bar{p}$ collisions at $\sqrt{s} = 1.8$ TeV. Such correlations are expected to arise from b quark hadronization and from B^{**} decays. We partially reconstruct B mesons using the semileptonic decays $B^0 \rightarrow \ell^+ D^{(*)-} X$ and $B^+ \rightarrow \ell^+ \bar{D}^0 X$. From the oscillation frequency, we obtain the mass difference between the two B^0 mass eigenstates, $\Delta m_d = 0.471_{-0.068}^{+0.078}(\text{stat}) \pm 0.034(\text{syst}) \hbar \text{ ps}^{-1}$, and measure the efficiency and purity of this flavor tagging method for both charged and neutral B mesons.

PACS numbers: 13.20.He, 14.40.Nd

The B^0 meson is a bound state of a \bar{b} quark and a d quark. Second order electroweak processes in which $\bar{b} \rightarrow \bar{d}$ while $d \rightarrow b$ result in the transition of B^0 mesons into \bar{B}^0 mesons and thus $B^0 \leftrightarrow \bar{B}^0$ oscillations. The $b \rightarrow d$ coupling occurs via a virtual top quark, thus the frequency of these oscillations is sensitive to the magnitude of the element V_{td} of the Cabibbo-Kobayashi-Maskawa matrix [1]. For an initially pure sample of B^0 mesons (at $t = 0$), the numbers of B^0 (N_+) and \bar{B}^0 (N_-) mesons at proper time t are given by

$$N_{\pm}(t) = N_+(0) \frac{e^{-t/\tau}}{2} (1 \pm \cos \Delta m_d t), \quad (1)$$

where τ is the lifetime of the B^0 meson and Δm_d is the mass difference between the mass eigenstates of the B^0 - \bar{B}^0 system. In this paper we determine Δm_d by measuring the fre-

quency of $B^0 \leftrightarrow \bar{B}^0$ flavor oscillations using partially reconstructed semileptonic decays of the B meson to $\ell D^{(*)}X$. The data used in this analysis were collected with the Collider Detector at Fermilab (CDF), at the Tevatron $p\bar{p}$ Collider at $\sqrt{s} = 1.8$ TeV, and correspond to an integrated luminosity of ~ 110 pb $^{-1}$.

To extract Δm_d the proper time of the B decay is required, as well as the flavor of the B meson at the times of its decay and production. While the B flavor at decay is determined by its decay products, the determination of the initial B flavor is experimentally challenging. Techniques to determine the initial B flavor in several previous measurements of Δm_d [2] relied on identifying the flavor from the other b hadron in the event (*e.g.*, using the lepton charge from the semileptonic decay of this other hadron), and are thus referred to as Opposite Side Tagging (OST).

It has been suggested [3] that the electric charge of particles produced near a B meson could also be used to determine its initial flavor, providing a basis for Same Side Tagging (SST). For example, if a \bar{b} quark combines with a u quark to form a B^+ meson the remaining \bar{u} quark may combine with a d quark to form a π^- (Throughout this paper, reference to a specific particle state implies the charge conjugate state as well). Similarly, if a \bar{b} quark hadronizes to form a B^0 meson, the associated pion would be a π^+ . Another source of correlated pions are decays of the orbitally excited ($L = 1$) B mesons (B^{**}) [4], *i.e.*, $B^{**0} \rightarrow B^{(*)+}\pi^-$ or $B^{**+} \rightarrow B^{(*)0}\pi^+$. In a hadron collider experiment with central rapidity coverage such as CDF, SST methods are attractive since they are expected to have significantly higher efficiency than the OST methods. These methods can also be used for measurements of CP violation [5].

In this paper we extract Δm_d by applying an SST method to a sample of events containing a lepton and a reconstructed D meson from B decay. To determine the initial flavor of the B meson, we select one charged track that we will generically refer to as a ‘‘pion’’, and use its charge as a tag. We do not attempt to distinguish the hadronization pions from those originating from B^{**} decays. The lepton charge tags the B -flavor at decay time. We classify the B - π combinations as right-sign (RS: $B^+\pi^-$ and $B^0\pi^+$) or wrong-

sign (WS: $B^+\pi^+$ and $B^0\pi^-$). We form the asymmetry in the RS and WS combinations, $\mathcal{A}(ct) \equiv (N_{RS}(ct) - N_{WS}(ct))/(N_{RS}(ct) + N_{WS}(ct))$, as a function of the proper decay length ct . For B^+ mesons, we expect an asymmetry independent of ct : $\mathcal{A}^+(ct) = \text{constant} \equiv \mathcal{D}_+$. The quantity \mathcal{D}_+ is called the dilution and it is a direct measure of the SST purity, *i.e.*, $(1 + \mathcal{D})/2$ is the fraction of correctly tagged events. Due to $B^0\bar{B}^0$ mixing, $\mathcal{A}(ct)$ for the neutral B mesons will vary as a function of the proper decay length ct . From eq. (1) and the definition of the B^0 asymmetry, it follows that the latter is expected to oscillate as $\mathcal{A}^0(ct) = \mathcal{D}_0 \cdot \cos(\Delta m_d t)$. Mistags, *i.e.*, incorrect flavor determinations, result in a decrease of the oscillation amplitude by the B^0 dilution factor \mathcal{D}_0 . We measure the asymmetry as a function of the proper decay length ct for both B^+ and B^0 mesons, and fit them with their expected time dependence, obtaining Δm_d , \mathcal{D}_0 and \mathcal{D}_+ . Ref. [6] discusses several effects that can result in $\mathcal{D}_0 \neq \mathcal{D}_+$, and in this analysis we impose no constraints on their relative values.

The CDF detector is discussed in detail elsewhere [7], and only the features most relevant to this analysis are described here. In CDF, the positive z axis is pointed in the proton direction, θ is the polar angle and ϕ is the azimuthal angle. The pseudorapidity, η , is defined as $-\ln[\tan(\theta/2)]$. We use two devices inside a 1.4 T solenoid to measure tracks from charged particles: the central tracking chamber (CTC) and the silicon vertex detector (SVX). The combined CTC+SVX tracking system covers the pseudorapidity interval $|\eta| < 1.1$, and gives a resolution on the transverse momentum with respect to the beam axis, p_T , of $\delta(p_T)/p_T = ((0.0066)^2 + (0.0009p_T)^2)^{1/2}$ and a resolution on the track impact parameter, d_0 , defined as the distance of closest approach to the beamline, of about $(13 + 40/p_T) \mu\text{m}$, where p_T is in GeV/c . Electromagnetic (CEM) and hadronic (CHA) calorimeters are located outside the solenoid and are surrounded by the central muon chambers (CMU) followed by the central upgrade muon chambers (CMP).

The data were recorded using an inclusive lepton (e and μ) trigger. The E_T threshold for the single electron trigger was 8 GeV, where $E_T \equiv E \sin \theta$, and E is the energy measured in the CEM. The single muon trigger required a charged track with $p_T > 7.5 \text{ GeV}/c$ in the CTC with matched track segments in both the CMU and CMP systems. Details of the

identification of electrons and muons are described in references [8] and [9].

We use the decay chains $B^0 \rightarrow \nu\ell^+D^{(*)-}$, with $D^- \rightarrow K^+\pi^-\pi^-$, or $D^{*-} \rightarrow \bar{D}^0\pi_*^-$ followed by \bar{D}^0 decaying to $K^+\pi^-$, $K^+\pi^-\pi^+\pi^-$, or $K^+\pi^-\pi^0$, where π_*^- denotes the low-momentum (soft) pion from the D^{*-} decay. We use $B^+ \rightarrow \nu\ell^+\bar{D}^0$, with $\bar{D}^0 \rightarrow K^+\pi^-$, where the \bar{D}^0 is required not to form a D^{*-} candidate with another π candidate in the event. We reconstruct the D meson candidates using tracks in a circle of unit radius in η - ϕ space around the lepton. For details, see [10]. We use only tracks that include SVX information. The decay products from the D mesons are required to be significantly displaced from the interaction point (primary vertex) of the event. The mass distributions of the four decay signatures with fully reconstructed D mesons are shown in Fig. 1a, b and c, while the distribution of $\Delta m = m(K\pi\pi_*) - m(K\pi)$ for the signature with $D^{*-} \rightarrow \bar{D}^0\pi_*^-$, followed by $\bar{D}^0 \rightarrow K^+\pi^-\pi^0$ (the π^0 is not reconstructed) is displayed in Fig. 1d.

To select the SST pion, we consider all tracks that are within the circle in η - ϕ space of radius 0.7 centered around the direction of the B meson, approximated by $\vec{p}(\ell) + \vec{p}(D)$. SST candidate tracks should originate from the B production point (the primary vertex of the event), and are therefore required to satisfy $d_0/\sigma_{d_0} < 3$, where σ_{d_0} is the uncertainty on d_0 . String fragmentation models [11] indicate that particles produced in the b -quark hadronization chain have low momenta transverse to the direction of the b -quark momentum. We thus select as the tag the track that has the minimum component of momentum, p_T^{rel} , orthogonal to the momentum sum of the track and the B meson. We define the tagging efficiency, ϵ , as the fraction of B candidates with at least one track satisfying the above requirements. We measure $\epsilon \approx 70\%$, independent of the decay signature used. On average, there are about 2.2 SST candidate tracks per B candidate.

For each of the five decay signatures, we subdivide the candidates into six bins in proper decay length, ct . The measurement of ct begins with finding the D decay vertex. The D candidate trajectory is intersected with the lepton track (and the momentum of π_* from the D^* , if present) to form the B decay vertex. We define L_{xy}^B to be, in the plane transverse to the beam axis, the distance between the primary and the B vertex projected along the B -

momentum vector. We estimate p_T^B from the p_T of the visible decay products, $p_T^{\ell D} = |\vec{p}_T(\ell) + \vec{p}_T(D^{(*)})|$, and the mean of the distribution of the momentum ratio $\mathcal{K} \equiv \langle p_T^{\ell D}/p_T^B \rangle$ obtained from a Monte Carlo simulation [12]. The $p_T^{\ell D}/p_T^B$ distribution has a mean of $\sim 85\%$ and RMS of $\sim 12\%$. The proper decay length of the B meson is then given by $ct = L_{xy}^B(m_B/p_T^{\ell D})\mathcal{K}$ [13].

We measure the asymmetry $\mathcal{A}^{(m)}(ct)$, in each ct bin by simultaneously fitting the mass distributions for candidates tagged with a RS or WS pion. The measured asymmetries are shown in Fig. 2. If the $\ell^+\bar{D}^0$ and $\ell^+D^{(*)-}$ signatures were pure signals of B^+ and B^0 decays, we could simply extract Δm_d using the time-dependence of $\mathcal{A}^0(ct)$. However, the signatures are mixtures of B^+ and B^0 decays, and thus $\mathcal{A}^{(m)}(ct)$ is a linear combination of the true asymmetries $\mathcal{A}^0(ct)$ and $\mathcal{A}^+(ct)$. To extract Δm_d , \mathcal{D}_0 and \mathcal{D}_+ , it is necessary to determine the *sample composition* of each $\ell^+D^{(*)}$ signature, by which we mean the fractions of the $\ell^+D^{(*)}$ candidates originating from the decays of the B^0 and B^+ mesons. Because a B^+ is associated with a π^- , whereas an unmixed B^0 is associated with a π^+ , the observed asymmetries are reduced by cross-contamination. To obtain the true asymmetries \mathcal{A}^0 and \mathcal{A}^+ , we introduce sample composition parameters (f^{**} , P_V , ξ_{norm} , R_f , $\epsilon(\pi_*)$, and τ_{B^+}/τ_{B^0} , defined below) to describe this cross-contamination and vary these parameters in a simultaneous fit to all of the observed asymmetries.

Cross-contamination can arise if the soft pion π_*^- from the D^{*-} decay is not identified – the decay sequence $B^0 \rightarrow \nu\ell^+D^{*-}$ will be reconstructed as $\ell^+\bar{D}^0$, that is, as a B^+ candidate. We quantify this effect by the efficiency for reconstructing the soft pion, $\epsilon(\pi_*)$. We determine $\epsilon(\pi_*)$ by comparing the fraction, R^* , of all $\ell^+\bar{D}^0X$ candidates for which we find a π_*^- candidate, with the prediction from the other sample composition parameters. (The final result is $\epsilon(\pi_*) = 0.85 \pm 0.07$). Since \bar{D}^{*0} does not decay to $D^-\pi^+$, there is no cross-contamination from $B^+ \rightarrow \nu\ell^+\bar{D}^{*0}$ into the B^0 sample.

Another source of cross-contamination arises from semileptonic B decays involving P -wave D^{**} resonances as well as non-resonant $D^{(*)}\pi$ pairs, which cannot be easily recognized and removed from the sample. For example, the decay sequence $B^0 \rightarrow \nu\ell^+D^{*-}$, followed by $D^{*-} \rightarrow \bar{D}^0\pi_{**}^-$ (where by π_{**} we denote the pion originating from D^{**} decay) will be

reconstructed as $\ell^+\bar{D}^0$, because of the missed π_{**}^- ; again, a B^0 decay is misclassified as a B^+ candidate. We quantify this effect by the parameter f^{**} , which is the ratio of the branching fraction $\mathcal{B}(B \rightarrow \nu\ell D^{**})$ to the inclusive semileptonic B branching fraction, $\mathcal{B}(B \rightarrow \ell\nu X)$. We use $f^{**} = 0.36 \pm 0.12$ [14]. The fractions of B^+ and B^0 decays in each decay signature are also affected by the relative abundance of the four possible spin-parity D^{**} states, some of which decay only to $D^*\pi$ and others to $D\pi$. We define $P_V = \mathcal{B}(B \rightarrow D^{**} \rightarrow D^*\pi) / [\mathcal{B}(B \rightarrow D^{**} \rightarrow D^*\pi) + \mathcal{B}(B \rightarrow D^{**} \rightarrow D\pi)]$, which we leave as a free parameter in our fit.

The sample composition also depends on f and f^* , the ratios of the branching fractions $B \rightarrow \nu\ell D$ and $B \rightarrow \nu\ell D^*$ to the inclusive semileptonic B branching fraction. We define $R_f \equiv f^*/f$, use $R_f = 2.5 \pm 0.6$ [15], and assume $f + f^* + f^{**} = 1$. The lifetime ratio τ_{B^+}/τ_{B^0} is another sample composition parameter: $\tau_{B^+} \neq \tau_{B^0}$ implies $\mathcal{B}(B^+ \rightarrow \ell^+\nu X) \neq \mathcal{B}(B^0 \rightarrow \ell^+\nu X)$, as well as a ct -dependent sample composition. We use $\tau_{B^+}/\tau_{B^0} = 1.02 \pm 0.05$ [15].

The tagging is further complicated when a π_{**}^\pm from D^{**} decay is present. The π_{**}^\pm may be incorrectly selected as the SST pion, always resulting in a RS correlation. The requirement $d_0/\sigma_{d_0} < 3$ reduces this effect: the π_{**} originates from the B meson *decay* point, whereas the appropriate tagging track originates from the B meson *production* point. The contamination of the tagging pions from π_{**}^\pm decreases with increasing ct . It is quantified by the parameter ξ , defined as the probability of selecting the π_{**} as the tag in a tagged event in which a π_{**}^\pm was produced. We use a Monte Carlo simulation [16] of b quark fragmentation and decay to determine ξ as a function of proper decay time. We then use our data to determine a normalization factor for ξ , ξ_{norm} , from the fraction, R^{**} , of all tagged events in which a π_{**} was selected as the tag. We measure R^{**} from the distribution of impact parameter, d_B , of the SST pion with respect to the B decay point. In this study, the $d_0/\sigma_0 < 3$ requirement was removed to increase the number of events. We fit the RS distribution of d_B/σ_{d_B} with the sum of the scaled WS distribution and a Gaussian of unit width centered at zero. The area of this Gaussian yields the total number of SST pions originating from D^{**} decays. We extract ξ_{norm} by comparing R^{**} with the prediction from the other sample composition

parameters. We measure separate values of R^{**} for ℓD and ℓD^* signatures, and their ratio constrains P_V . ($\xi_{norm} = 0.8 \pm 0.2$ and $P_V = 0.3 \pm 0.3$ are the final results).

The mass difference Δm_d and the dilutions \mathcal{D}_0 and \mathcal{D}_+ are determined from a χ^2 fit to the measured asymmetries $\mathcal{A}^{(m)}$. In the fit, f^{**} , R_f and τ_{B^+}/τ_{B^0} vary within their uncertainties, while $\epsilon(\pi_*)$, P_V , and ξ_{norm} vary within constraints imposed through the measured values of R^* and R^{**} . The prediction for an observed B^0 asymmetry is

$$\bar{\mathcal{A}}_k = \alpha_k^0 \mathcal{A}^0 + \alpha_k^+ (-\mathcal{A}^+) + \alpha_k^{**} (+1) \quad (2)$$

where all information about the sample composition is contained in the coefficients $\alpha_k^{0,+}$ [13]. The second term in (2) describes the cross-contamination occurring with the minus sign due to the opposite charge correlation for B^+ , while the third term describes the effect of selecting the π_{**}^\pm as a tag.

The result of the fit, overlaid onto the measured asymmetries, is displayed in Fig. 2. The oscillation in the neutral B signatures is clearly present, giving $\Delta m_d = 0.471 \text{ } \hbar \text{ ps}^{-1}$. The fit has a χ^2 of 26.5 for 30 degrees of freedom. We assign the uncertainties from the sample composition parameters, which are dominated by the uncertainty on f^{**} , to the systematic uncertainties on Δm_d , \mathcal{D}_0 or \mathcal{D}_+ . Other sources of systematic uncertainty are much smaller, and are due to uncertainties in the Monte Carlo simulation as well as the presence of physics background processes that can mimic the $\ell^+ D^{(*)} X$ signatures. The systematic uncertainties are given in Table I. The final result for the mixing frequency is $\Delta m_d = 0.471_{-0.068}^{+0.078}(\text{stat}) \pm 0.034(\text{syst}) \text{ } \hbar \text{ ps}^{-1}$. We also obtain the following values for the neutral and charged meson tagging dilutions: $\mathcal{D}_0 = 0.18 \pm 0.03(\text{stat}) \pm 0.02(\text{syst})$ and $\mathcal{D}_+ = 0.27 \pm 0.03(\text{stat}) \pm 0.02(\text{syst})$. The fit indicates that $\sim 82\%$ of the $\ell^+ \bar{D}^0 X$ signature comes from B^+ decays, while $\sim 80\%$ of the $\ell^+ D^- X$ and $\sim 95\%$ of the $\ell^+ D^{*-} X$ originate from B^0 . The B^0 component of the $\ell^+ \bar{D}^0 X$ signature can be seen as a small anti-oscillation in Fig. 2, top.

In conclusion, we have applied a Same Side Tagging technique to samples of $B^0 \rightarrow \ell^+ D^{(*)-} X$ and $B^+ \rightarrow \ell^+ \bar{D}^0 X$ decays in $p\bar{p}$ collisions. The measurement of the asymmetry

between tag-charge and B -flavor as a function of proper time for neutral B mesons results in the observation of a time-dependent oscillation $B^0 \leftrightarrow \bar{B}^0$, with the oscillation frequency $\Delta m_d = 0.471_{-0.068}^{+0.078}(\text{stat}) \pm 0.034(\text{syst}) \hbar \text{ ps}^{-1}$, in good agreement with the world average $\Delta m_d = 0.474 \pm 0.031 \hbar \text{ ps}^{-1}$ [15]. This establishes the effectiveness of Same Side Tagging for the first time in hadronic collisions.

We thank the Fermilab staff and the technical staffs of the participating institutions for their vital contributions. This work was supported by the U.S. Department of Energy and the National Science Foundation; the Italian Istituto Nazionale di Fisica Nucleare; the Ministry of Education, Science and Culture of Japan; the Natural Sciences and Engineering Research Council of Canada; the National Science Council of the Republic of China; and the A.P. Sloan Foundation.

- [1] N. Cabibbo, Phys. Rev. Lett **10**, 531 (1963); M. Kobayashi and K. Maskawa, Prog. Theor. Phys. **49**, 652 (1973).
- [2] For a recent review of experimental results on $B^0\bar{B}^0$ oscillations see O. Schneider, 18th International Symposium on Lepton-Photon Interactions, Hamburg, Germany, 1997, to appear in the proceedings.
- [3] M. Gronau, A. Nippe and J. Rosner, Phys. Rev. D **47**, 1988 (1993).
- [4] P. Abreu *et al.*, Phys. Lett. B **345** 598 (1995); R. Akers *et al.*, Z. Phys. C **66**, 19 (1995); D. Buskulic *et al.*, Z. Phys. C **69**, 393 (1996);
- [5] *The CDF II Detector Technical Design Report*, FERMILAB-Pub-96/390-E.
- [6] I. Dunietz and J. L. Rosner, Phys. Rev D **51**, 2471 (1995).
- [7] F. Abe *et al.*, Nucl. Instr. Meth. A **271**, 387 (1988), and references therein. The SVX is described in F. Abe *et al.*, Phys. Rev. D **50**, 2966 (1994).

- [8] F. Abe *et al.*, Phys. Rev. Lett. **71**, 500 (1993).
- [9] F. Abe *et al.*, Phys. Rev. Lett. **71**, 3421 (1993).
- [10] F. Abe *et al.*, Phys. Rev. Lett. **76**, 4462 (1996).
- [11] B. Andersson, G. Gustafson, G. Ingelman and T. Sjöstrand, Phys. Rep. **97**, 31 (1983).
- [12] We generate B mesons according to the model described by P. Nason, S. Dawson and R. K. Ellis, Nucl. Phys. B **327**, 49 (1988). We simulate B -meson decays using QQ, P. Avery, K. Read and G. Trahern, Cornell Internal Note CSN-212, March 25, 1985 (unpublished). We use version 9.1.
- [13] P. Maksimović, Ph.D. dissertation, Massachusetts Institute of Technology, 1997 (unpublished).
- [14] R. Fulton *et al.*, Phys. Rev. D **43**, 651 (1991).
- [15] R. M. Barnett *et al.*, Phys. Rev. D **54**, 1 (1996).
- [16] We use PYTHIA, H.-U. Bengtsson and T. Sjöstrand, Comput. Phys. Commun. **46**, 43 (1987). The version 5.7 was used. We simulate B -meson decays using the QQ package [12].

Source	$\sigma(\mathcal{D}_+)$	$\sigma(\mathcal{D}_0)$	$\sigma(\Delta m_d)(\hbar \text{ ps}^{-1})$
Composition	+0.0216 -0.0131	+0.0225 -0.0131	+0.0295 -0.0310
Other sources	± 0.0068	± 0.0074	± 0.0146
Total	+0.0226 -0.0147	+0.0237 -0.0150	+0.0329 -0.0343

TABLE I. The breakdown of the systematic uncertainties.

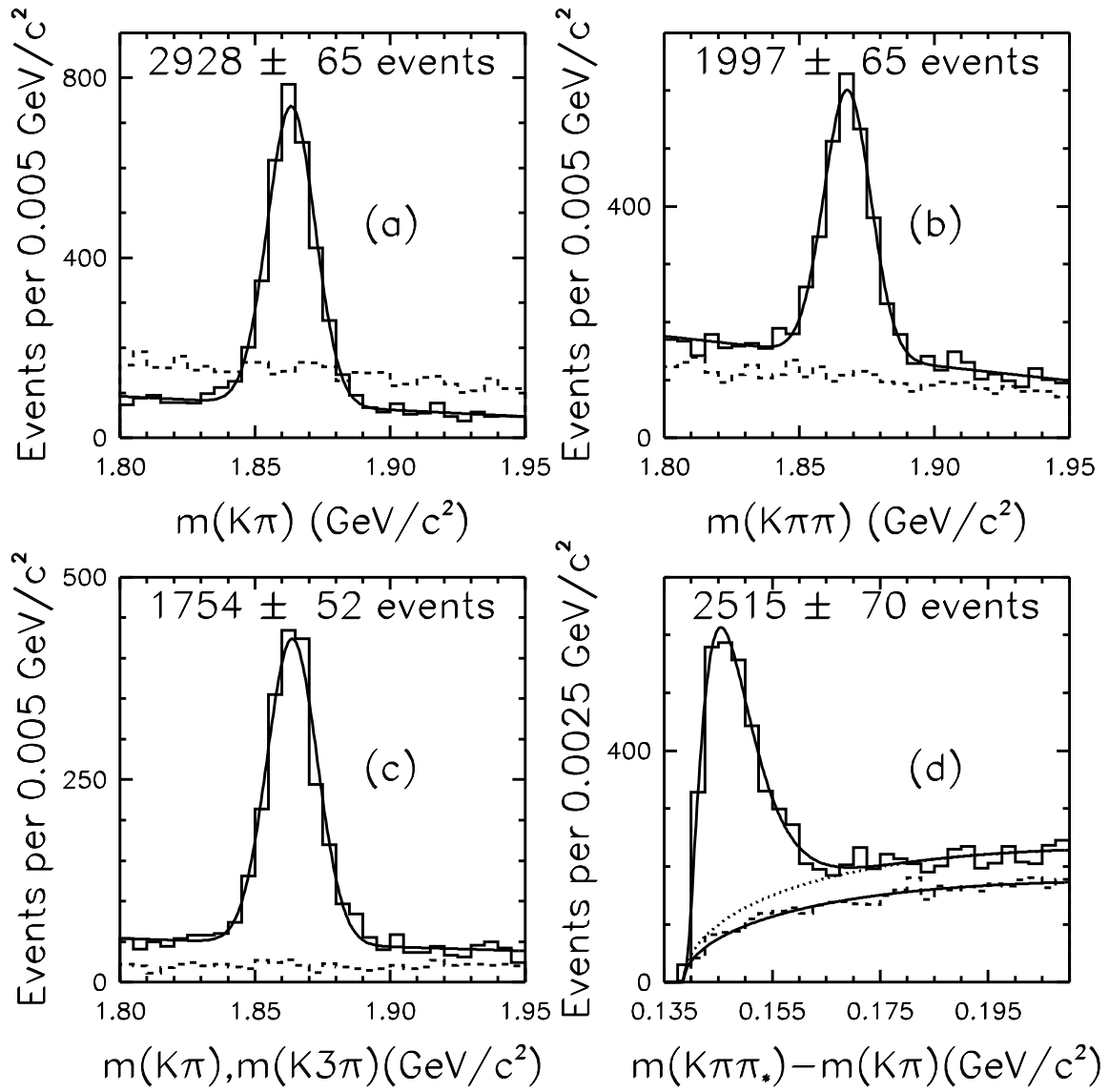


FIG. 1. Invariant mass distributions of the five $B \rightarrow \ell^+ D^{(*)} X$ signatures used in the analysis. The solid histograms correspond to the “right” lepton-kaon charge correlation ($\ell^+ K^+$), and the dashed histograms the “wrong” one ($\ell^+ K^-$). The solid lines are the fits to the $\ell^+ K^+$ distributions, and the resulting number of signal events is given on each figure. (a) $K^+ \pi^-$ mass in $\ell^+ \bar{D}^0 X$ ($\bar{D}^0 \rightarrow K^+ \pi^-$). (b) $K^+ \pi^- \pi^-$ mass in $\ell^+ D^- X$ ($D^- \rightarrow K^+ \pi^- \pi^-$). (c) \bar{D}^0 candidate mass in $\ell^+ D^{*-} X$ ($D^{*-} \rightarrow \bar{D}^0 \pi_*^-$, $\bar{D}^0 \rightarrow K^+ \pi^-$ and $\bar{D}^0 \rightarrow K^+ \pi^- \pi^+ \pi^-$). (d) $K^+ \pi^- \pi_*^- - K^+ \pi^-$ mass difference in $\ell^+ D^{(*)-} X$ ($D^{*-} \rightarrow \bar{D}^0 \pi_*^-$, $\bar{D}^0 \rightarrow K^+ \pi^- \pi^0$). The $\ell^+ K^+$ background shape (dotted line) was determined from the fit (lower solid curve) of the $\ell^+ K^-$ distribution.

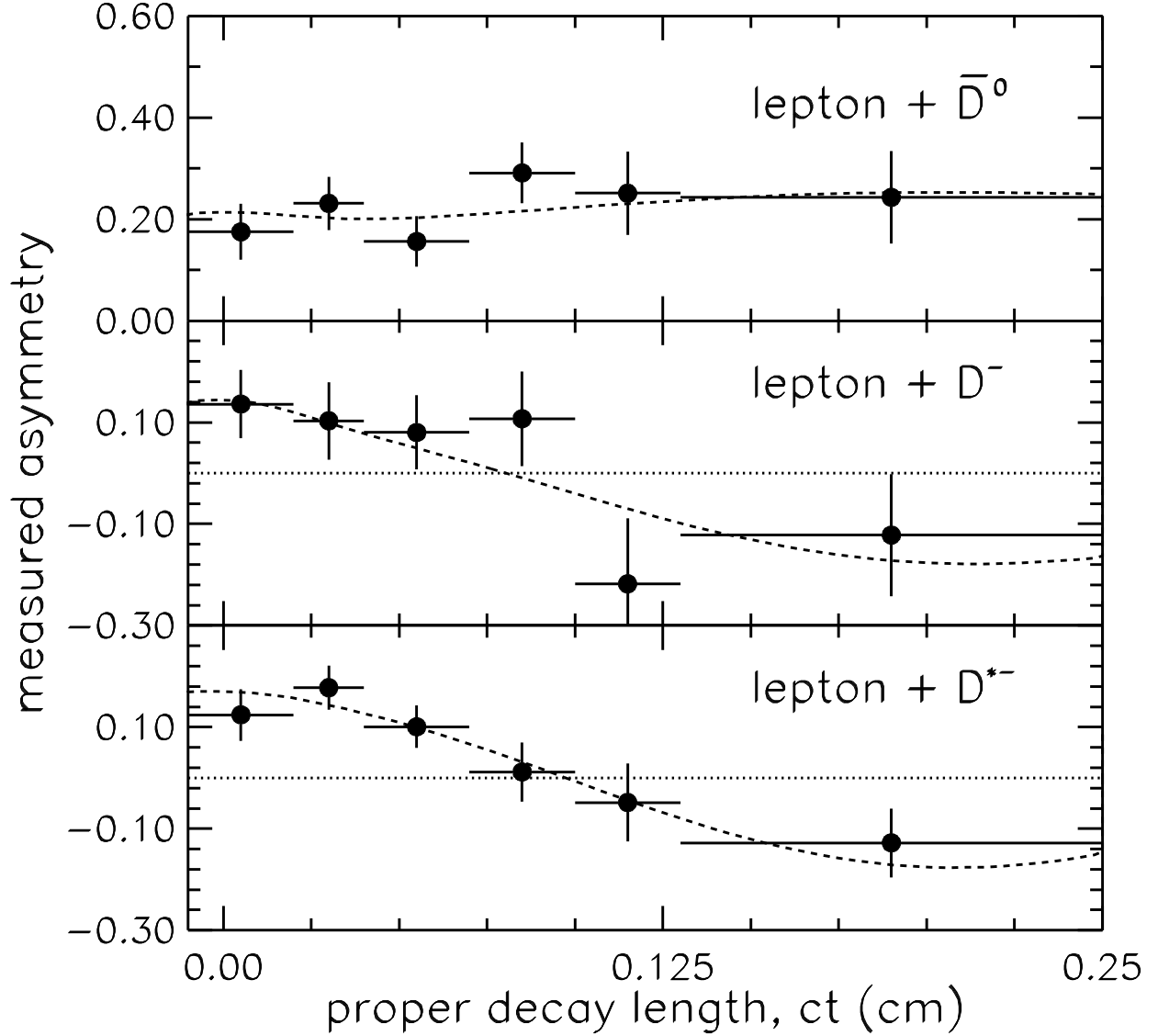


FIG. 2. Measured asymmetries as a function of the proper decay length, ct , for the decay signatures: $\ell^+ \bar{D}^0$ (dominated by B^+), $\ell^+ D^-$ and the sum of all three $\ell^+ D^{*-}$ (dominated by B^0). We fit the three $\ell^+ D^{*-}$ signature separately, but combine them for display purposes. The dashed line is the result of the fit.